Comparison of Gafchromic EBT2 and EBT3 films for clinical photon and proton beams

S. Reinhardt[a)]
Fakultät für Physik, Ludwig-Maximilians Universität München, 85748 Garching, Germany

M. Hillbrand[b)]
Rinecker Proton Therapy Center, 81371 München, Germany

J. J. Wilkens
Department of Radiation Oncology, Technische Universität München, Klinikum rechts der Isar, 81675 München, Germany

W. Assmann
Fakultät für Physik, Ludwig-Maximilians Universität München, 85748 Garching, Germany

(Received 7 March 2012; revised 5 July 2012; accepted for publication 5 July 2012; published 1 August 2012)

Purpose: Dose verification in highly conformal radiation therapy such as IMRT or proton therapy can benefit from the high spatial resolution offered by radio-chromic films such as Gafchromic EBT or EBT2. Recently, a new generation of these films, EBT3, has become available. The composition and thickness of the sensitive layer are the same as for the previous EBT2 films. The most important change is the symmetric layer configuration to eliminate side orientation dependence, which is reported for EBT2 films.
Methods: The general film characteristics such as sensitivity to read-out orientation and postexposure darkening evolution of the new EBT3 film are evaluated. Film response has been investigated in clinical photon and proton beams and compared to former EBT2 films. Quenching effects in the proton Bragg peak region have been studied for both, EBT2 and EBT3 films.
Results: The general performance of EBT3 is comparable to EBT2, and the orientation dependence with respect to film side is completely eliminated in EBT3 films. Response differences of EBT2 and EBT3 films are of the same order of magnitude as batch-to-batch variations observed for EBT2 films. No significant difference has been found for both generations of EBT films between photon and proton exposure. Depth dose measurements of EBT2 and EBT3 show an excellent agreement, though underestimating dose by up to 20% in the Bragg peak region.
Conclusions: The symmetric configuration of EBT3 presents a major improvement for film handling. EBT3 has similar dosimetric performance as its precursor EBT2 and can, thus, be applied to dose verification in IMRT in the same way. For dose verification in proton therapy the underresponse in the Bragg peak region has to be taken into account. © *2012 American Association of Physicists in Medicine*. [http://dx.doi.org/10.1118/1.4737890]

Key words: Gafchromic film, EBT2 film, EBT3 film, energy dependence, depth dose curve, proton therapy

I. INTRODUCTION

Intensity modulation, whether applied with conventional photon (IMRT) or actively scanned proton beams (IMPT), is in daily clinical use in modern radiation oncology. Complex radiation fields are applied to optimize the dose to the three-dimensional tumor volume, while at the same time minimizing side effects to surrounding healthy tissue. Patient specific quality assurance (QA) measurements are of particular importance to ensure the adequate quality of beam delivery for such complex and highly conformal intensity modulated treatment techniques. Use of diode or ionization chamber arrays for QA in IMRT is limited in regions of high dose gradients due to the mm to cm spacing of individual detector elements. Gafchromic EBT (Gafchromic® EBT self-developing film for radiotherapy dosimetry, International Speciality Products), a self-developing radio-chromic film, offers sensitivity in the 0.1–10 Gy dose range, a nearly water-equivalent effective atomic number ($Z_{eff}^{EBT} = 6.84$ compared to $Z_{eff}^{water} = 7.3$) (Ref. 1) and sub-mm spatial resolution, when read-out by conventional flatbed scanners.[2] Furthermore, films can be handled in visible light and the possibility to immerse films in water for short periods of time allows their use in water phantoms. Today, EBT has been completely replaced by EBT2 films (Gafchromic® EBT2 self-developing film for radiotherapy dosimetry, International Specialty Products). Recently, the third generation of EBT films, EBT3, has become available (EBT3 product information, International Speciality Products). Both successive EBT types have the same radiation sensitive component as the original EBT film. However, since the introduction of EBT2 films, a yellow marker dye is incorporated in the active layer for uniformity corrections.

 0094-2405/2012/39(8)/5257/6/$30.00

Furthermore, the double active layer structure of EBT has been replaced by a single sensitive layer. EBT as well as EBT2 film were shown to be well adapted for IMRT QA in regions of high dose gradients, showing only weak energy dependence for clinically relevant photon and electron energies.[1,3]

Dose verification with high spatial accuracy is also of particular interest in proton therapy where the combination of active scanning of small pencil beams and the characteristic Bragg curve with well-defined particle ranges allows high dose conformity to the target volume. Gafchromic films are, therefore, also candidates for high resolution dose verification in proton beams. However, radio-chromic films are known to underestimate dose in the Bragg peak region.[4–7] Measuring of quenching effects in the vicinity of the Bragg peak is thus mandatory before these films can be used in proton dosimetry.

The aim of our study was to measure film response to photon and proton exposure as well as quenching effects in the Bragg peak region for the newly introduced EBT3 films. For comparison, the same measurements have been accomplished using the EBT2 film. Additionally, some general aspects of EBT3 film performance such as uniformity, orientation sensitivity, and postexposure density growth are presented. Similar studies on energy dependence and film performance comparing EBT and EBT2 have been accomplished in the past.[8–11]

II. MATERIAL AND METHODS

II.A. Gafchromic EBT2 and EBT3 films

Incident radiation initiates a solid-state polymerization within the sensitive layer of radio-chromic films, resulting in a characteristic dose-dependent film darkening. All generations of Gafchromic EBT film incorporate the lithium salt of pentacosa-10,12-diynoate (LiPAD) as active monomer.[12] Due to the hair-like structure of the active component and its preferential orientation, film response in flatbed scanner-based dosimetry strongly depends on the film orientation with respect to the scanning direction.[13] EBT2 films have a single active layer of 30 μm nominal thickness. The sensitive layer is asymmetrically placed between a polyester substrate of 175 μm and 80 μm of different protective cover layers. This nonsymmetric layer configuration introduced a further orientation dependent effect, yielding response deviations for the same scanning orientation when different sides of the film are facing the scanner.[14,15] EBT3 films offer a symmetrical layer configuration, which is claimed to eliminate such side orientation effects. The composition of the sensitive layer as well as nominal layer thickness is the same as for EBT2. The active layer is symmetrically sandwiched between two 125 μm thick polyester laminates with a special surface treatment to prevent the formation of Newton rings during film scanning.[12]

II.B. Experimental setup

Two different batches of EBT2 (F06110902, A07160902) and a single batch of EBT3 (A11021102) films have been investigated. After May 2009 EBT2 film composition was standardized.[10] Hence, homogeneity problems related to early batches of EBT2 (Ref. 16) are not relevant for the lots used within this work.

Films were cut into pieces of 50 × 50 mm^2 prior to exposure and marked to ensure retention of scanner orientation throughout all experiments. From each sheet used for calibration or energy dependence measurements some film pieces were left unexposed for background determination.

For response measurements, each film batch was exposed to different dose levels in the range of 0.2–8.0 Gy, with dose steps ΔD of 0.5 Gy except for proton calibration of EBT2 films, where dose steps of 1.0 Gy were used. Films were irradiated with 6 MV photons at the isocenter of a clinical linear accelerator (Varian Clinac DHX, Varian Medical Systems, Inc., Palo Alto, CA), at a depth of 17 mm in a PMMA phantom (300 × 300 × 30 mm^3). A field size of 40 × 40 mm^2 was used. Proton irradiation was accomplished at the Rinecker Proton Therapy Centre (RPTC) in Munich. A proton pencil beam with a nominal energy of 228 MeV (Gaussian shape of 4 mm sigma, 328.0 mm range in water) was actively scanned to deliver a homogeneous dose to a single layer of 50 × 50 mm^2. Spot weights were equally distributed and the lateral spot spacing was set to 5 mm. Films were placed in a PMMA phantom (300 × 300 × 300 mm^3) at a depth of 50 mm in the plateau region of the Bragg curve. No quenching effects are expected for the residual energy of 203 MeV at the film position, which corresponds to a water-equivalent depth of 61 mm according to our regular calibration measurements. A rigid stem ionization chamber and a 0.125 cm^3 Semiflex Chamber connected to a Unidos Electrometer (all PTW, Freiburg, Germany) were used for reference dosimetry in the photon and proton beam, respectively. Films were placed in the same depth as the chamber reference point. Chamber readings were corrected according to the TRS 398 for temperature, pressure, and beam quality.[17] All other correction factors, e.g., such as for recombination, have been neglected. However, the accuracy in dose determination is assumed to be better than ± 3% for dose response measurements and both radiation types.

The proton depth dose distribution was measured in a solid-water phantom (RW3, PTW, Freiburg, Germany), allowing mm-resolution of the Bragg peak of the incident 200 MeV proton beam assuming an initial energy spread (sigma) of better 1 MeV. Films were placed perpendicular to the beam direction into the phantom. The water equivalent scattering and attenuation properties of the films allow simultaneous irradiation of multiple film pieces at different depths. The same field size (50 × 50 mm^2) as for dose response measurements was employed. For analysis, the film position was expressed in terms of water-equivalent thickness by converting film and phantom thickness based on their specific mass density.

In addition, films have been exposed to a ^{90}Sr-source, yielding dose levels of 3.2, 6.2, and 9.0 Gy, to measure the postexposure optical density growth over a time period of 52 h.

After irradiation, exposed as well as unexposed film pieces for background correction were stored together in a light-tight envelope at room temperature. Films were scanned

48 ± 1 hour after irradiation with an Epson Perfection V700 Photo scanner (EPSON Deutschland GmbH, Meerbusch, Germany) in transmission mode. The scanner software "EPSON Scan" provided with the scanner was used in professional mode, with all available image correction methods turned off. Five preview scans were taken before the start of film scanning to allow the scanner temperature to stabilize and, thus, prevent any temperature dependent response effects. Films were placed in the middle of the scan window, where no correction of scan field uniformity is required, and scanned in landscape orientation with the full physical resolution of 1200 dpi. The higher resolution compared to the commonly used 72 dpi was chosen in order to apply the calibrated films for dose verification in small-field cell and mouse tumor irradiation experiments.[18] Obtained 48-bit RGB-images were saved in the uncompressed tagged image file format.

For film analysis, raw pixel values from the red color channel (PVR) are converted into a net optical density value (netOD),

$$\text{netOD} = \text{OD}_{\text{irradiated}} - \text{OD}_{\text{unirradiated}} = -\log_{10}\frac{\text{PVR}_{\text{irradiated}}}{\text{PVR}_{\text{unirradiated}}}.$$

As region of interest for film analysis, a central film area of 2.5 × 2.5 mm^2 (3.2 × 3.2 mm^2) was chosen for exposed (unexposed) films, respectively. While the ROI size in case of exposed films was limited by the uniformity and flatness of the irradiated areas, a larger ROI was chosen for unexposed films to obtain higher statistics in uniformity measurements.

III. RESULTS

III.A. EBT3 performance

Pixel values of the red color channel of 20 unirradiated film pieces of a single EBT3 film sheet were analyzed to test film uniformity. For all film pieces, the standard deviation of pixel values was below 1.2%, the standard deviation of the mean value of all film pieces was even below 0.2%.

Dependence on film orientation with respect to film side as well as scanning orientation was investigated for films exposed to dose levels of 0.5 Gy, 1.0 Gy, 3.0 Gy, and 5.1 Gy and 6 pieces of unirradiated films (Fig. 1). A similar sensitivity to the scanning direction was found as known for both former film types, EBT and EBT2.[13,19] Deviations with respect to the film side facing the scan window do not exceed 0.8% (0.9%) in terms of pixel values (dose) for all investigated dose levels. Uniformity of exposed films was found to be on average better than 1.5%.

Postexposure growth of film darkening of 6%–9% within 24 h after irradiation was reported for EBT2 films.[8] EBT3 film shows a similar film darkening with time as EBT2, yielding an average increase in film darkening within 24 h of 7.6% for all investigated dose levels, which corresponds to an increase in measured dose of 11.7%. However, for an accuracy in dose determination better 1%, a time window for scanning after 24 h of ±3h has been obtained.

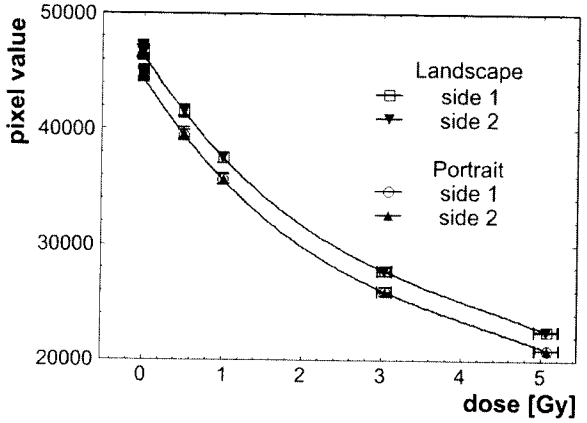

FIG. 1. EBT3 film sensitivity with respect to scanning and side orientation for different dose levels from photon exposure. Lines are shown to guide the eye. Side dependency is negligible for EBT3 films, while significant differences with respect to scanning direction (landscape, portrait) are present.

III.B. Film response measurements

A comparison of dose response curves of different EBT2 film batches and a single EBT3 film lot is depicted in Fig. 2 where dose D is plotted against netOD. The uncertainty in netOD corresponds to the standard deviation of the mean netOD value in the analyzed ROI, which has been found to be on average 3.5% for all dose response curves. Dose errors are associated with the accuracy of reference dosimetry, which was assumed to be better than ±3%. Response curves have been fit according to Ref. 20 by the following equation:

$$D = A_0 \cdot \text{netOD} + A_1 \cdot \text{netOD}^{A_2}.$$

Fit parameters A_i ($i = 0 \ldots 2$) are given in Table I. Dose uncertainties related to fit parameters are typically 3% for the used calibration fit, although fit uncertainties of up to 6% have been observed for EBT2 film calibration with protons. These elevated fit uncertainties are attributed to fewer sampling points of the calibration curves. Accounting for an additional uncertainty in netOD of about 1%, an overall accuracy in dose determination better than 4% can be obtained for all

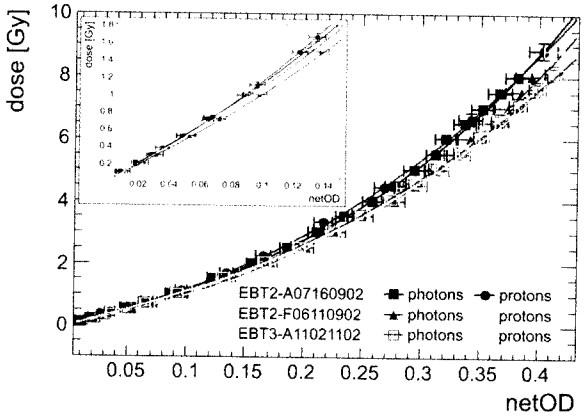

FIG. 2. NetOD response to clinical proton and photon beams for different batches of EBT2 and EBT3 films. Response deviations from batch-to-batch exceed deviations related to different radiation types. Lines correspond to fits. The inset shows zoomed image for dose range 0–2Gy.

TABLE I. Fit parameters of dose response curves.

Film lot	Radiation type	Fit parameter		
		A_0 [Gy]	A_1 [Gy]	A_2
F06110902	Photon	9.35 ± 0.27	60.93 ± 3.87	2.9
	Proton	8.32 ± 0.44	49.91 ± 4.97	2.6
A07160902	Photon	10.44 ± 0.30	59.53 ± 3.61	2.8
	Proton	9.93 ± 0.52	42.47 ± 4.25	2.4
A11021102	Photon	10.08 ± 0.37	37.75 ± 2.43	2.5
	Proton	9.90 ± 0.35	38.02 ± 2.51	2.6

films and radiation types except for the proton calibration of EBT2 films due to the smaller sampling rate in this specific experiment.

For all investigated dose levels of a single film batch, differences in netOD response with respect to radiation type are below 6%, thus showing only a weak dependence on radiation type. For EBT2 films, batch-to-batch response is considerably different, for instance, for a netOD of 0.15, dose deviations of both lots of 14.6% and 12.3% are obtained for photon and proton irradiation, respectively. Comparison of EBT2 and EBT3 response for the same netOD yields a difference of 13.7% for photons and 8.7% for protons. Deviations are, therefore, of the same order of magnitude as batch-to-batch variations of EBT2 films.

III.C. Proton depth dose measurements

Depth dose curves measured by EBT2 and EBT3 films are shown in Fig. 3 together with the depth dose curve provided by the clinical treatment planning system used as reference. There is an excellent agreement of EBT2 and EBT3 depth dose curves over the whole proton range. Reference and film curves comply with each other in the plateau region, while both films show an underestimation of dose in the Bragg peak, as already reported for the older EBT films.[6,7,21] This can be seen better by plotting the relative deviation $\Delta D_{film\text{-}TPS}$ of

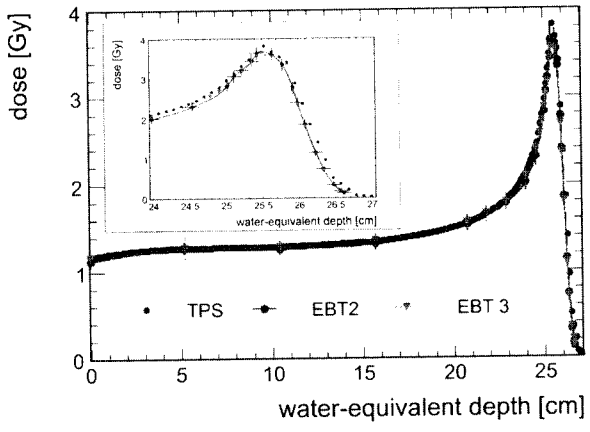

FIG. 3. Comparison of proton depth dose measurements (initial energy = 200 MeV) using EBT2 and EBT3 films with reference data of the planning system (TPS). Lines are applied as guide to the eye. There is no significant difference between EBT2 and EBT3 films, both showing an average underresponse of up to 5% for energies below 40 MeV and up to 20% in the vicinity of the Bragg peak, corresponding to the lowest residual energy of 4 MeV.

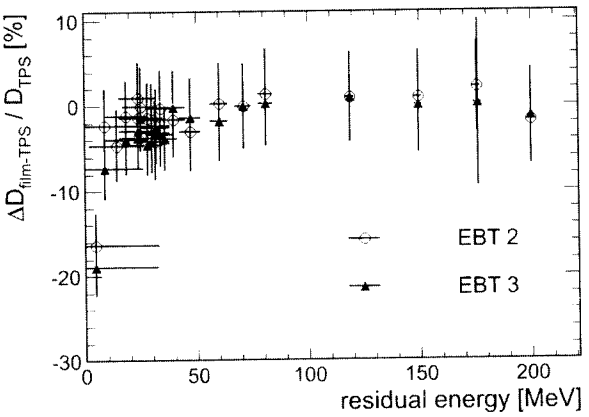

FIG. 4. Relative deviation of film dose and reference dose are within measurement uncertainties for all residual energies exceeding 20 MeV. LET dependence becomes visible for residual proton energies below 15 MeV.

film measurement (D_{Film}) and reference curve (D_{TPS}) against residual proton energy (Fig. 4),

$$\Delta D_{film-TPS}(E) = \frac{(D_{film}(E) - D_{TPS}(E))}{D_{TPS}(E)} \cdot 100\%.$$

The residual energy was determined according to the range-energy relationship of Ref. 22. The parameters $\alpha = 0.0022$ cm/MeV^p and $p = 1.77$ were taken from, Ref. 22 R_0 and z correspond to proton range and phantom depth, respectively,

$$E(z) = \frac{1}{\alpha^{1/p}(R_0 - z)^{1/p}}.$$

The uncertainty in residual energy was calculated by error propagation, accounting for range straggling (expressed by the range straggling approximation given in Ref. 22 as an upper bound used at all depths, including the initial energy spread of the beam) as well as a measurement uncertainty in depth of ±1%. No significant difference in LET dependence of EBT2 and EBT3 films can be deduced from the data. For all energies down to about 15 MeV, film and reference dose agree within ±5%. At lower energies, the film show an underresponse of the dose, which increases with decreasing proton energy up to about 20% for the lowest available energy.

IV. DISCUSSION

Unirradiated as well as irradiated EBT3 films show a uniformity better 1.5%, which is in good agreement with film specifications. It is well known that film orientation with respect to scan direction is an important issue for scanner-based film read-out due to response differences of landscape and portrait orientation. EBT3 shows significant response differences for both scan orientations in accordance to previous generations of EBT films. Hence, the recommendation to maintain for all measurements the same orientation as during calibration also holds for the new EBT3 films. Side orientation sensitivity of the former EBT2 film introduced another orientation related potential source of systematic error in scanner-based film dosimetry. Deviations with respect to

film side are found to be well below 1% for EBT3 films, and, thus, within the typical statistical spread of pixel values. Hence, side sensitivity is completely eliminated by the symmetrical layer configuration of EBT3. Furthermore, a clear reduction of Newton ring formation has been observed during film scanning, confirming the manufacturer's specification. The reduction of Newton ring formation is achieved by silica particles incorporated in the polyester substrate, which introduce a small air gap ($\sim 5\ \mu$m) between film and scanner glass. Furthermore, differences in the average physical density of EBT3 compared with EBT2 are of the order of 10^{-3}g/cm^3.[23] Within our measurement accuracy no significant effect of this air-silica-particle layer with respect to spatial resolution, film uniformity or dose response has been found. Any effect is, therefore, clinically not relevant.

EBT2 and EBT3 films have the same sensitive component as well as thickness. Differences in atomic composition of the active layer of EBT2 and EBT3 films are below 0.1% and, therefore, negligibly small.[24] Hence, no significant radiation type dependence of film response has been seen for all investigated film lots. Dose response curves for photons and protons of single film batches agree within ±5% in the clinical relevant dose range up to 3 Gy (Fig. 3). This observation agrees with results recently published for EBT and EBT2 films, comparing photon and proton response curves.[1,25] Furthermore, good agreement of film darkening evolution of EBT3 and EBT2 films has been found.

Average batch-to-batch variations of up to 12% are significantly large and confirm the need to recalibrate films of each new lot.

For instance, for EBT2, a measured netOD of 0.15 yields dose deviations of 14.6% and 12.3% for photon and protons, respectively, when using calibration curves of different batches. Comparing deviations of proton and photon calibration curves of the same lot for a netOD of 0.15 yields dose errors below 1.5% for EBT2 and below 4.6% for EBT3. An uncertainty in sensitive layer thickness of ±10% from batch-to-batch is given by the manufacturer for both, EBT2 as well as EBT3 films. Assuming similar inner-batch thickness uncertainties of up to 3% as for EBT,[26] all observed response differences with respect to film batch are of the order of thickness variation within the active layer.

For EBT, an under response of about 10% for an average proton energy of 3.2 MeV is reported, obtained from depth dose measurements in a 15 and 29 MeV proton beam.[6] For EBT2 (EBT3) films a mean under response of 3% (5%) in the Bragg peak region ($E < 40$ MeV) and up to 17% (19%) for the lowest measured residual energy of 4 MeV has been measured for an incident 200 MeV proton beam (Fig. 4). However, care has to be taken when comparing energy quenching related to different initial beam energies, as energy spread and LET at a certain depth depends on the initial proton energy.

The high LET proton proportion within the energy spectrum is responsible for the quenching effects observed for average residual energies below 15 MeV (Fig. 4). Quenching effects increase with decreasing residual proton energy as energy spread and energy loss straggling increase.

No LET dependence is observed in the depth dose measurement for residual proton energies exceeding 20 MeV. This is consistent with results published for EBT films, comparing LET dependence of proton beams in the 50–200 MeV range.[25]

V. CONCLUSION

EBT3 films show an excellent uniformity and similar darkening time evolution as EBT2 films. The side orientation sensitivity of previous EBT2 films has been completely eliminated for EBT3 films due to the symmetric configuration, though scanning orientation still has to be maintained.

EBT3 films show the same dosimetric response to photon and proton beams as its predecessor EBT2. No dependence on radiation type has been found for the investigated film batches, except for protons in the vicinity of the Bragg peak. Hereby, care has to be taken due to a considerable dose underresponse of the film. Further research is necessary to quantify the impact on dose measurements.

As EBT3 has shown to offer the same dosimetric properties as EBT2, the same protocols established for EBT2 film dosimetry can, therefore, be applied to EBT3 films. All in all, EBT3 as well as their predecessor are valuable tools for dose verification measurements when high spatial resolution is required.

ACKNOWLEDGMENT

Supported by DFG Cluster of Excellence: Munich-Centre for Advanced Photonics. The authors want to state that no actual or potential conflicts of interest exist.

[a]Electronic mail: Sabine.Reinhardt@physik.uni-muenchen.de; Telephone: +49 89-289-14283.
[b]Author to whom correspondence should be addressed. Electronic mail: Martin.Hillbrand@rptc-1.de; Telephone +49 89-72467-0.

[1] B. Arjomandy *et al.*, "Energy dependence and dose response of Gafchromic EBT2 film over a wide range of photon, electron and proton beam energies," Med. Phys. **37**(5), 1942–1947 (2010).
[2] O. Hupe and J. Brunzendorf, "A novel method of radiochromic film dosimetry using a color scanner," Med. Phys. **33**(11), 4085–4094 (2006).
[3] M. Todorovic *et al.*, "Evaluation of Gafchromic EBT prototype B for external beam dose verification," Med. Phys. **33**(5), 1321–1328 (2006).
[4] S. M. Vatnisky, "Radiochromic film dosimetry for clinical proton beams," Appl. Radiat. Isot. **48**(5), 643–651 (1997).
[5] A. Piermattei *et al.*, "Radiochromic film dosimetry of a low energy proton beam," Med. Phys. **27**(7), 1655–1660 (2000).
[6] D. Kirby *et al.*, "LET dependence of GafChromic films and ion chamber in low-energy proton dosimetry," Phys. Med. Biol. **55**, 417–433 (2010).
[7] L. Zhao and I. J. Das, "Gafchromic EBT film dosimetry in proton beams," Phys. Med. Biol. **55**, N291–N301 (2010).
[8] C. Andres *et al.*, "A comprehensive study of the Gafchromic EBT2 radiochromic film: A comparison with EBT," Med. Phys. **37**(12), 6271–6278 (2010).
[9] S. Devic *et al.*, "Absorption spectra time evolution of EBT2-model Gafchromic® film," Med. Phys. **37**(5), 2207–2214 (2010).
[10] P. Lindsay *et al.*, "Investigation of energy dependence of EBT and EBT-2 Gafchromic film," Med. Phys. **37**(2), 571–576 (2010).
[11] J. G. H. Sutherland and D. W. O. Rogers, "Monte Carlo calculated absorbed-dose energy dependence of EBT and EBT2 film," Med. Phys. **37**(3), 1110–1116 (2010).

[12]D. F. Lewis, *Gafchromic Film*, 2010 (available URL: http://online1.ispcorp.com/en-US/gafchromic/Pages/ProductDetail.aspx?BU=GafChromi&prdId=41046).
[13]M. J. Butson, T. Cheung, and P. K. N. Yu, "Scanning orientation effects on Gafchromic EBT film dosimetry," Australas. Phys. Eng. Sci. Med. **29**(3), 281–284 (2006).
[14]J. Desroches, H. Bouchard, and F. Lacroix, "Potential errors in optical density measurements due to scanning side in EBT and EBT2 Gafchromic film dosimetry," Med. Phys. **37**(4), 1565–1570 (2010).
[15]D. F. Lewis, *Using Radiochromic Film*, 2010 (available URL: http://online1.ispcorp.com/en-US/gafchromic/Pages/ProductDetail.aspx?BU=GafChromic&prdId=41046).
[16]B. Hartmann, M. Mártisìková, and O. Jäkel, "Homogeneity of Gafchromic® EBT2 films," Med. Phys. **37**(4), 1753–1756 (2010).
[17]IAEA, "Absorbed dose determination in external beam radiotherapy: An international code of practice for dosimetry based on standards on absorbed dose to water," Technical Report Series No. 398 (IAEA, Vienna 2000).
[18]C. Greubel *et al.*, "Scanning irradiation device for mice in vivo with pulsed and continuous proton beams," Radiat. Environ. Biophys. **50**(3), 339–344 (2011).
[19]S. Saur and J. Frengen, "Gafchromic EBT film dosimetry with flatbed CCD scanner: A novel background correction method and full dose uncertainty analysis," Med. Phys. **35**(7), 3094–3101 (2008).
[20]S. Devic *et al.*, "Dosimetric properties of improved GafChromic films for seven different digitizers," Med. Phys. **31**(9), 2392–2401 (2004).
[21]B. Arjomandy *et al.*, "EBT2 film as a depth-dose measurement tool for radiotherapy beams over a wide range of energies and modalities," Med. Phys. **39**(2), 912–921 (2012).
[22]T. Bortfeld, "An analytical approximation of the Bragg curve for therapeutic proton beams," Med. Phys. **24**(12), 2024–2033 (1997).
[23]D. F. Lewis (personal communication, 2012).
[24]C. Falk (personal communication, 2012).
[25]M. Martisikova and O. Jakel, "Dosimetric properties of Gafchromic (R) EBT films in monoenergetic medical ion beams," Phys. Med. Biol. **55**(13), 3741–3751 (2010).
[26]C. Falk (personal communication, 2009).